Arch. Pharm. Chem. Life Sci. 2016, *349*, 1–10

ARCH PHARM
Archiv der Pharmazie

Full Paper

Novel Tacrine-Based Pyrano[3′,4′:5,6]pyrano[2,3-*b*]quinolinones: Synthesis and Cholinesterase Inhibitory Activity

Roshanak Hariri[1], Zahra Afshar[1], Mohammad Mahdavi[2], Maliheh Safavi[3], Mina Saeedi[4,5], Zahra Najafi[6], Reyhaneh Sabourian[5], Elahe Karimpour-Razkenari[5], Najmeh Edraki[7], Farshad Homayouni Moghadam[8], Abbas Shafiee[1], Mahnaz Khanavi[9], and Tahmineh Akbarzadeh[1,5]

[1] Faculty of Pharmacy, Department of Medicinal Chemistry, Tehran University of Medical Sciences, Tehran, Iran
[2] Drug Design and Development Research Center, Tehran University of Medical Sciences, Tehran, Iran
[3] Department of Biotechnology, Iranian Research Organization for Science and Technology, Tehran, Iran
[4] Medicinal Plants Research Center, Faculty of Pharmacy, Tehran University of Medical Sciences, Tehran, Iran
[5] Persian Medicine and Pharmacy Research Center, Tehran University of Medical Sciences, Tehran, Iran
[6] Faculty of Pharmacy, Department of Medicinal Chemistry, Hamadan University of Medical Sciences, Hamadan, Iran
[7] Medicinal and Natural Products Chemistry Research Center, Shiraz University of Medical Sciences, Shiraz, Iran
[8] Department of Cellular Biotechnology at Cell Science Research Center, Royan Institute for Biotechnology, ACECR, Isfahan, Iran
[9] Faculty of Pharmacy, Department of Pharmacognosy, Tehran University of Medical Sciences, Tehran, Iran

In order to develop effective anti-cholinesterase compounds, a novel series of pyrano[3′,4′:5,6]-pyrano[2,3-*b*]quinolinones were designed, synthesized, and evaluated *in vitro* against acetylcholinesterase (AChE) and butyrylcholinesterase (BChE). All derivatives showed very good AChE inhibitory (AChEI) activity ($IC_{50} = 0.37–5.62\ \mu M$) compared with rivastigmine ($IC_{50} = 11.07\ \mu M$). Among them, 11-amino-12-(2,3-dichlorophenyl)-3-methyl-7,8,9,10-tetrahydropyrano[3′,4′:5,6]pyrano[2,3-*b*]quinolin-1(12*H*)-one (**6f**) displayed the best inhibitory activity. However, most of the synthesized compounds showed no anti-BChE activity and compounds **6b** and **6f** were found to be only moderate inhibitors. The most potent anti-AChE compound **6f** had low and moderate inhibitory activity and neuroprotective effects against beta-secretase (BACE1) and oxidative stress-induced cell death, respectively. Also, kinetic and molecular docking studies of binding interactions elucidated that compound **6f** bound to both the catalytic anionic site (CAS) and peripheral anionic site (PAS) of AChE.

Keywords: Acetylcholinesterase / Alzheimer's disease / Butyrylcholinesterase / Fused heterocycles / Pyrano[3′,4′:5,6]pyrano[2,3-*b*]quinolinones

Received: April 25, 2016; Revised: October 12, 2016; Accepted: October 13, 2016

DOI 10.1002/ardp.201600123

Additional supporting information may be found in the online version of this article at the publisher's web-site.

Correspondence: Dr. Tahmineh Akbarzadeh, Faculty of Pharmacy, Department of Medicinal Chemistry, Tehran University of Medical Sciences, Tehran, Iran.
E-mail: akbarzad@tums.ac.ir
Fax: +98-21-66461178

Introduction

Alzheimer's disease (AD) has emerged as the most common age-related neurodegenerative disorder [1]. It is categorized as one of the top ten causes of death in the United States.

ARCH PHARM
Archiv der Pharmazie

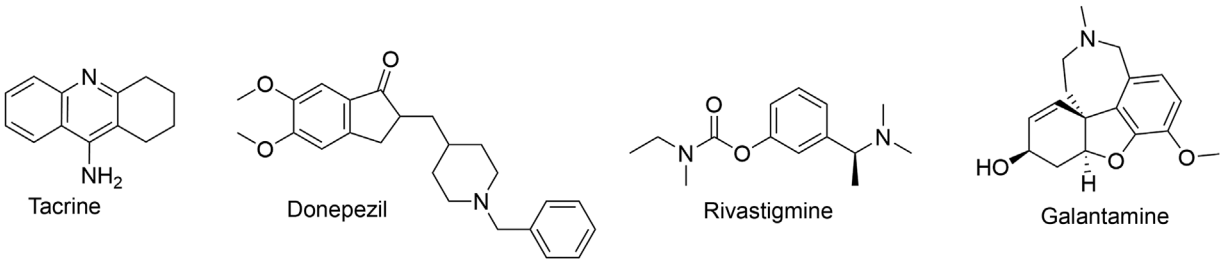

Figure 1. Structures of four approved ChEI drugs.

Although several reasons such as genetic, environmental, and endogenous factors are associated with AD, decrease of acetylcholine (ACh) is the main cause of AD [2] leading to cognitive and memory symptoms [3].

Acetylcholinesterase (AChE) and butyrylcholinesterase (BChE) are two enzymes which lyse choline-based esters. Thus, inhibition of AChE and BChE improves the symptoms in patients with AD. In a healthy brain, AChE activity is significant and predominates over BChE activity (as a pseudocholinesterase or nonspecific cholinesterase). Also, it has been revealed that AChE is mainly found in neurons while BChE is generally present in plaques and tangles in glial cells [4]. Although most research on brain cholinesterases have been conventionally associated with AChE, important role of BChE in cholinergic neurotransmission and different nervous system dysfunctions has been well documented in the literature [5, 6]. In this regard, effective ChE inhibitors have been the center of attention as the key agents to enhance cholinergic transmission at cholinergic autonomic synapses as well as neuromuscular junction [7].

It has been proved that neurodegenerative diseases are also due to the accumulation of uncharacteristically folded β-amyloid peptide (Aβ) in the brains of patients, described by "Amyloid Cascade Hypothesis" theory [8]. It seems that the deposition of Aβ is the first pathological event which causes formation of senile plaques (SPs) followed by neurofibrillary tangles (NFTs) and death of neurons leading to AD. Thus, it is clear that inhibition of Aβ aggregation has been the masterwork for the treatment of AD [9]. Apart from these facts, noncholinergic role of AChE has been considered as a versatile reason for inducing SPs via accelerating Aβ deposition. It is supposed that AChE constructs a stable complex with SP components through its peripheral anionic site (PAS) [10, 11]. Therefore, AChEIs may increase not only cholinergic function, but also affect the generation of β-amyloid.

There are four approved ChEI drugs, tacrine, donepezil, rivastigmine, and galantamine (Fig. 1) and among them, tacrine (1,2,3,4-tetrahydroacridine-9-amine) is known as an effective AChEI and BChEI [12]. However, extensive use of tacrine was restricted since various side effects such as hepatoxicity were reported [13]. Hence, recent studies have been devoted to the design and synthesis of new and effective tacrine-based AChE inhibitors [14–20]. Herein, in continuation of our research program on the synthesis of anti-ChE compounds [19–25], we designed and synthesized novel tacrine analogs, pyrano[3′,4′:5,6]pyrano[2,3-*b*]quinolinone derivatives (Fig. 2).

Results and discussion

Chemistry

Synthetic route for the preparation of the desired pyrano-[3′,4′:5,6]pyrano[2,3-*b*]quinolinones **6a–o** is shown in Scheme 1. For this purpose, various 2-amino-4-aryl-7-methyl-5-oxo-4,5-dihydropyrano[4,3-*b*]pyran-3-carbonitriles **4a–o** were prepared by the reaction of 4-hydroxy-6-methyl-2*H*-pyran-2-one (**1**), aromatic aldehydes **2**, and malononitrile (**3**). Screening various commercially available basic reagents such as DABCO, NEt_3, K_2CO_3, and piperidine as well as different solvents (EtOH, MeOH, CH_3CN, $PhCH_3$, and CH_2Cl_2) in a model reaction revealed that using DABCO in EtOH at room temperature led to the formation of the corresponding products **4a–o** in good yields (80–85%). Then, reaction of compounds **4a–o** and cyclohexanone (**5**) was conducted in the presence of $AlCl_3$ in $ClCH_2CH_2Cl$ (DCE) under reflux conditions for 12–18 h to obtain the desired products **6a–o** in good yields (Table 1). The structure of all compounds was elucidated using IR, ^1H, and ^{13}C NMR spectroscopy as well as chemical analysis.

Pharmacology

Cholinesterase inhibitory activity

All synthesized pyrano[3′,4′:5,6]pyrano[2,3-*b*]quinolinones **6a–o** were evaluated for their cholinesterase inhibitory

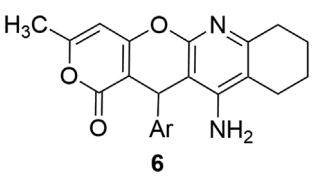

6

Figure 2. Structure of pyrano[3′,4′:5,6]pyrano[2,3-*b*]quinolinones **6**.

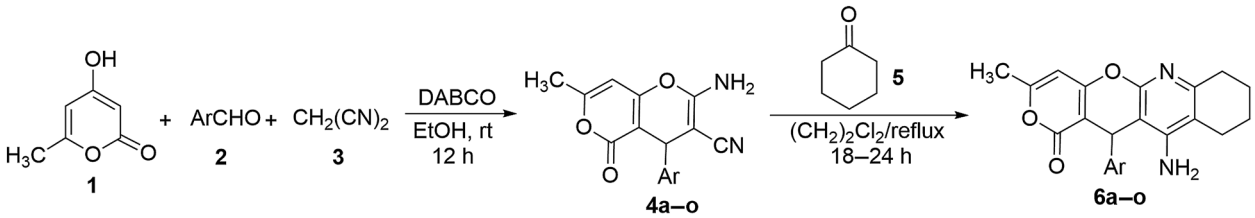

Ar = C_6H_5, 2-F-C_6H_4, 4-F-C_6H_4, 2-Cl-C_6H_4, 4-Cl-C_6H_4, 2,3-diCl-C_6H_3, 2-NO_2-C_6H_4, 3-NO_2-C_6H_4, 2-Me-C_6H_4, 3-Me-C_6H_4, 4-Me-C_6H_4, 4-MeO-C_6H_4, 3,4,5-triMeO-C_6H_2, 2-NO_2-5-Cl-C_6H_3, 2-Thiophenyl

Scheme 1. Synthesis of pyrano[3′,4′:5,6]pyrano[2,3-*b*]quinolinone derivatives **6**.

activity based on Ellman's modified procedure [20] (Table 1). All compounds showed very good anti-AChE activity (0.370–5.620 μM) comparing with rivastigmine as the reference drug (IC_{50} = 11.070 μM). They were also compared with tacrine (IC_{50} = 0.048 μM) in Table 1. Among the prepared derivatives, 11-amino-12-(2,3-dichlorophenyl)-3-methyl-7,8,9,10-tetrahydropyrano[3′,4′:5,6]pyrano[2,3-*b*]quinolin-1(12*H*)-one (**6f**) was the most potent compound toward AChE. Also, compounds **6n**, **6d**, and **6e** were found to be potent anti-AChE derivatives and IC_{50} values were obtained as 0.720, 0.800, and 0.820 μM, respectively. As can be seen in Table 1, compounds **6j**, **6k**, **6g**, and **6h** depicted good anti-AChE activity with IC_{50} = 1.170, 1.122, 1.234, and 1.259, respectively. Also, our results demonstrated that moderate activities were obtained

Table 1. Synthesis and IC_{50} values of pyrano[3′,4′:5,6]pyrano[2,3-*b*]quinolinones 6 against AChE and BChE.[a)]

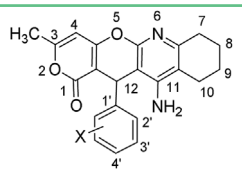

6a–o

Entry	Compound 6		AChE inhibition IC_{50} (μM)	BChE inhibition IC_{50} (μM)
1	**6a**	C_6H_5	1.940 ± 0.028	>50
2	**6b**	2-F-C_6H_4	1.870 ± 0.014	40.420 ± 0.019
3	**6c**	4-F-C_6H_4	4.100 ± 0.223	>50
4	**6d**	2-Cl-C_6H_4	0.800 ± 0.078	>50
5	**6e**	4-Cl-C_6H_4	0.820 ± 0.021	>50
6	**6f**	2,3-diCl-C_6H_3	0.370 ± 0.014	17.670 ± 0.429
7	**6g**	2-NO_2-C_6H_4	1.234 ± 0.099	>50
8	**6h**	3-NO_2-C_6H_4	1.259 ± 0.049	>50
9	**6i**	2-Me-C_6H_4	1.970 ± 0.042	>50
10	**6j**	3-Me-C_6H_4	1.170 ± 0.042	>50
11	**6k**	4-Me-C_6H_4	1.122 ± 0.042	>50
12	**6l**	4-MeO-C_6H_4	1.970 ± 0.049	>50
13	**6m**	3,4,5-triMeO-C_6H_2	2.970 ± 0.035	>50
14	**6n**	2-NO_2-5-Cl-C_6H_3	0.720 ± 0.007	>50
15	**6o**	2-Thiophenyl	5.620 ± 0.332	>50
16	Tacrine		0.048 ± 0.013	0.014 ± 0.009
21	Rivastigmine		11.070 ± 0.010	7.720 ± 0.020

[a)] Data are expressed as mean ± SE (three independent experiments).

by compounds **6b**, **6a**, **6l**, and **6m** ($IC_{50} = 1.870–2.970\ \mu M$). Compounds **6c** and **6o** were found to be the weakest inhibitors ($IC_{50} = 4.100$ and $5.620\ \mu M$) in comparison to other derivatives.

According to our results in Table 1, electronic properties of substituents as well as their positions on the aryl group at 12-position of compounds **6** played important role in AChEI activity. Compound **6f** having two chlorine atoms on the aryl ring showed the best inhibitory activity. Decreasing the number of chlorine atoms led to the reduction of inhibitory activity, which was confirmed by IC_{50} values obtained for compounds **6d** and **6e**. Nevertheless, compounds **6d** and **6e** did not show significant difference, indicating that the number of chlorine atoms was more important than their positions. It should be noted that the presence of an electron withdrawing group (NO_2) along with chlorine (compound **6n**) led to a potent anti-AChE activity; however, it was not as potent as compound **6f** having two chlorine atoms. Also, introduction of methyl (compounds **6j** and **6k**) or NO_2 (compounds **6g** and **6h**) groups into the various positions of aryl group induced good inhibitory activity. Comparing the corresponding results did not show remarkable anti-AChE activity since IC_{50} values were obtained in the range of $1.170–1.259\ \mu M$. It should be noted that the presence of 2-methylphenyl group did not induce potent inhibitory activity in compound **6i** ($IC_{50} = 1.970\ \mu M$) comparing with *meta* and *para* Me-substituted derivatives (**6j** and **6k**). Also, presence of strong electron donating group (OMe) on the aryl group of compound **6l** induced weaker inhibitory activity ($IC_{50} = 1.970\ \mu M$). Moreover, increasing the number of methoxy groups led to much weaker activity. Compounds **6a** and **6b** having phenyl and 2-flurophenyl groups showed activity with $IC_{50} = 1.940$ and $1.870\ \mu M$, respectively. It seems that the presence of fluorine at 2-pition of aryl group does not play important role in the inhibitory activity and introduction of fluorine into 4-position of aryl group induced much weaker activity in comparison to compounds **6a** and **6b**. Compound **6o** possessing 2-thienyl moiety was found to be the weakest anti-AChE compound ($IC_{50} = 5.620\ \mu M$).

Anti-BChE evaluation indicated that most of synthesized compounds **6a–o** induced no inhibitory activity toward BChE. Only compounds **6b** and **6f** showed BChEI activity with IC_{50} values of 40.420 and $17.670\ \mu M$, respectively. It is clear that compound **6f** was the most potent anti-ChE agent.

Kinetic studies

In order to reveal the inhibition mode of AChE induced by the most potent compound **6f**, a kinetics study was performed based on the modified Ellman's method [20]. As it is clear in Fig. 3, graphical analysis of the Lineweaver–Burk reciprocal plots demonstrated a mixed type of inhibition, confirming the fact that compound **6f** can bind to both the CAS and PAS of AChE. The inhibition constant ($K_i = 0.918\ \mu M$) was calculated using secondary replots of the slope versus concentrations of compound **6f**.

BACE1 enzyme inhibitory activity of compound 6f

Considering the fact that β-secretase (BACE1) plays significant role in AD pathogenesis, BACE-1 inhibitory activity of the most potent AChEI **6f** was evaluated via a fluorescence resonance energy transfer (FRET) based BACE-1 kit including BACE-1 enzyme and specific APP-based peptide substrate (Rh-EVNLDAEFK-quencher). Experiments were repeated for three times and compared with the reference compound OM99-2 (Table 2). Compound **6f** demonstrated low BACE1 inhibitory activity with percentage inhibition = 13.20 and 10.35 at 50 and $10\ \mu M$ of **6f**, respectively.

Neuroprotective effect of compound 6f against H_2O_2-induced cell death in PC12 neurons

The neuroprotective activity of compound **6f** was evaluated using PC12 cell line protocol to study neuronal

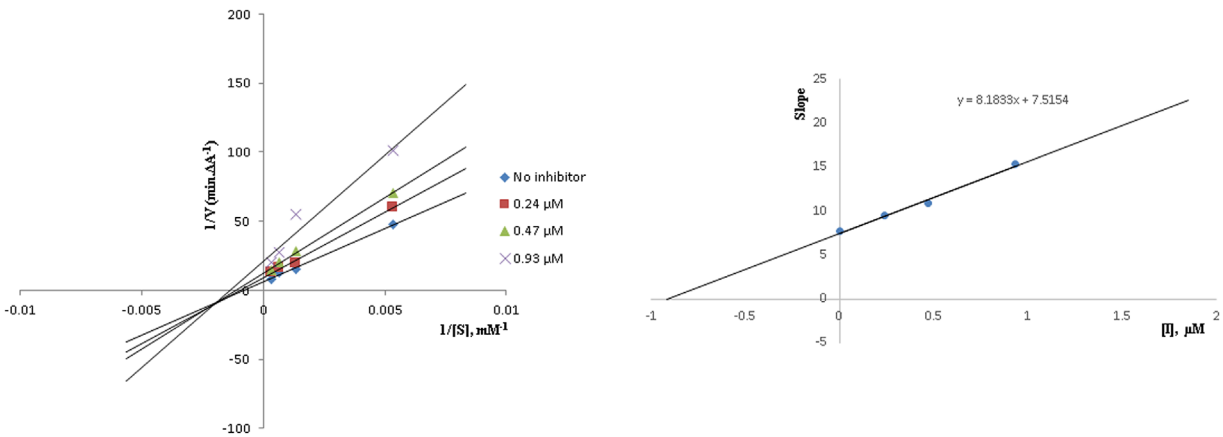

Figure 3. Left: Lineweaver–Burk plot for the inhibition of AChE by compound **6f** at different concentrations of acetylthiocholine (ATCh). Right: Steady-state inhibition constant (K_i) of compound **6f**.

Table 2. Inhibitory activity of compound 6f against BACE1 comparing with OM99-2.[a)]

Compound 6	Inhibition at 50 μM (%)[b)]	Inhibition at 10 μM (%)[b)]
6f	13.20 ± 1.94	10.35 ± 6.50

[a)] OM99-2 was tested at 10, 1, and 0.1 nM (IC_{50} = 0.014 ± 0.001 μM).
[b)] Values represent means ± standard error (S.E.) of three independent experiments.

differentiation [20]. In this respect, differentiated PC12 cells and H_2O_2 were considered as *in vitro* model and oxidative agent, respectively. Neuroprotective activity of compound **6f** was evaluated by subjecting PC12 cells to H_2O_2-induced damage comparing with quercetin. As depicted in Fig. 4, the percentage of cell viability was calculated in comparison to control group. Compound **6f** showed moderate neuroprotectivity at 100 μM (cell viability = 59.77% and $P < 0.0001$ vs. H_2O_2 treatment alone). It should be noted that compound **6f** demonstrated neuroprotectivity at 50 μM (cell viability = 54.25% with $P < 0.05$ vs. H_2O_2 treatment alone).

Molecular docking study

Docking study of the most active anti-AChE compound (**6f**) was performed to clarify the possible interactions between that compound and AChE. Compound **6f** possessing a chiral center at 12-position was prepared as a racemic mixture. In this respect, both (*R*)- and (*S*)-enantiomers were studied in docking simulations (Fig. 5). As can be seen in Fig. 6, the (*R*)-enantiomer occupied the peripheral anionic site (PAS) of AChE whereas the (*S*)-enantiomer was placed at the mid of the gorge of AChE interacting with both the PAS and CAS. The interaction between (*R*)-enantiomer and AChE demonstrated that 2,3-dichloroaryl moiety has oriented toward Leu282 and makes hydrophobic interaction (Fig. 6) whereas other parts of compound have oriented toward Tyr70, Tyr121, Tyr334, and Trp279 residues of the PAS. Also, it made π–π stacking interaction with Trp279 and hydrophobic interactions between cyclohexyl ring and Tyr334. The hydrogen bond between oxygen of pyran moiety and Tyr70 is another important interaction. All results confirmed that the compound has interacted with the PAS of AChE. Similarly (*S*)-enantiomer as depicted in Fig. 7, has located in the mid of the gorge of AChE. There are two π–π T-shaped interactions between heterocyclic moieties and Trp84 and His440 of the CS. It is clear that there are two π–π T-shaped interactions between pyridine moiety and Tyr334 and Phe331 of the PAS. Also, 2,3-dichloroaryl moiety has oriented toward Asp72 of the PAS and made anion-π interaction. However, hydrogen bond between nitrogen of pyridine moiety and Tyr121 of the PAS is significant.

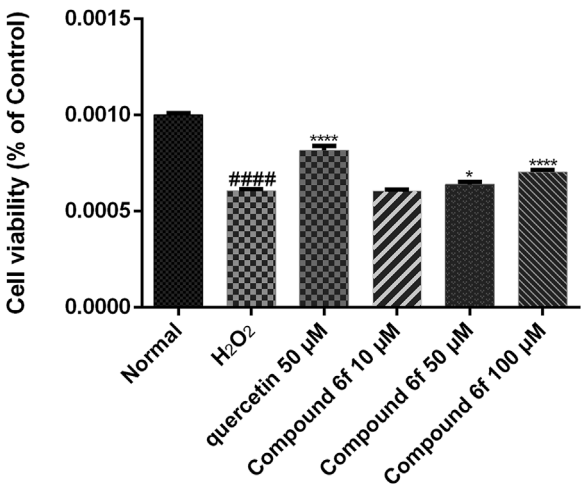

Figure 4. Neuroprotective effect of compound **6f** on cell viability of PC12 cells in H_2O_2-induced damage. Data are expressed as mean ± SD, and one-way analysis of variance (ANOVA) followed by Tukey's multiple comparisons test which was carried out to determine the level of significance. $^{###}P < 0.0001$ vs. control, $^{****}P < 0.0001$ vs. H_2O_2 and $^{*}P < 0.05$ vs. H_2O_2.

Conclusion

In conclusion, we designed, synthesized, and evaluated novel anti-ChE compounds, pyrano[3′,4′:5,6]pyrano[2,3-*b*]-quinolinones. The *in vitro* inhibitory activity revealed that 11-amino-12-(2,3-dichlorophenyl)-3-methyl-7,8,9,10-tetrahydropyrano[3′,4′:5,6]pyrano[2,3-*b*]quinolin-1(12*H*)-one (**6f**) having two chlorine atoms on the aryl moiety showed the best inhibitory activity toward both AChE and BChE. Although most of the synthesized compounds depicted good anti-AChE activity, the corresponding anti-BChE activities were not remarkable. Also, compound **6f** showed low and

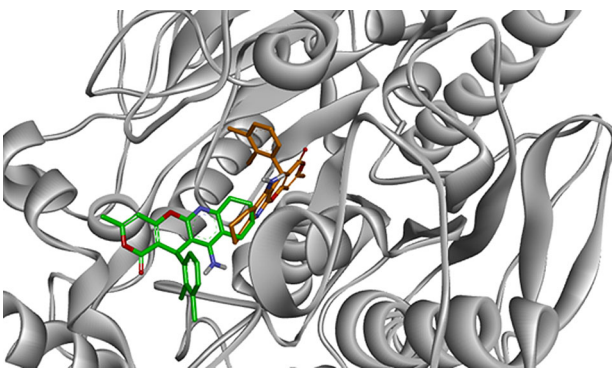

Figure 5. The proposed orientation of (*R*)- (green) and (*S*)-enantiomers (orange) of compound **6f** in the AChE.

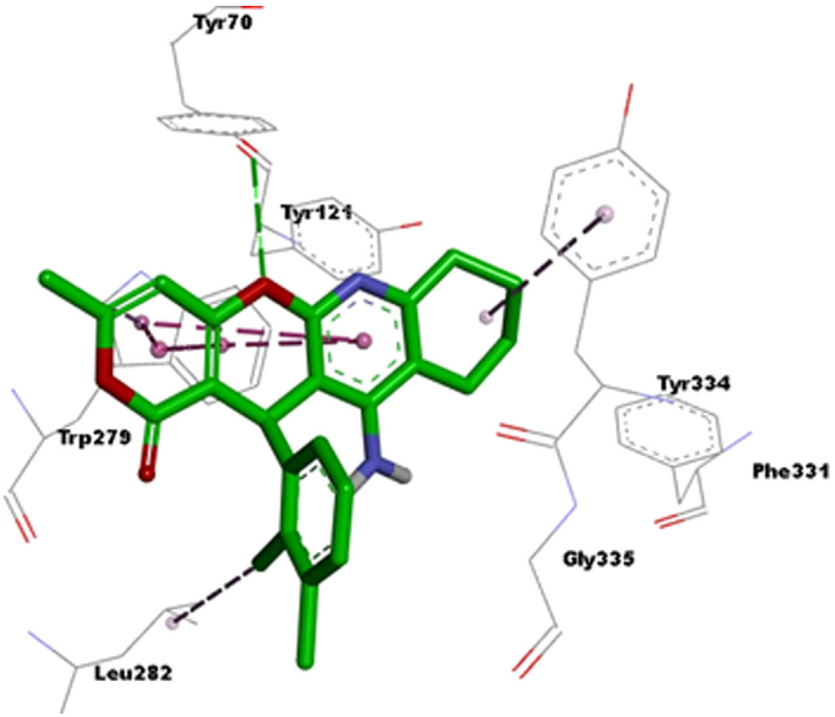

Figure 6. The binding mode of (*R*)-enantiomer (green) of compound **6f** in the active site of AChE.

moderate inhibitory activity and neuroprotective effects against beta secretase (BACE1) and oxidative stress-induced cell death, respectively. It should be noted that docking and kinetic studies confirmed that the inhibitory activity of the most potent compound **6f** spans both the CAS and PAS of AChE.

Experimental

Chemistry

General

Melting points were taken on a Kofler hot stage apparatus and are uncorrected. ^{1}H and ^{13}C NMR spectra were recorded

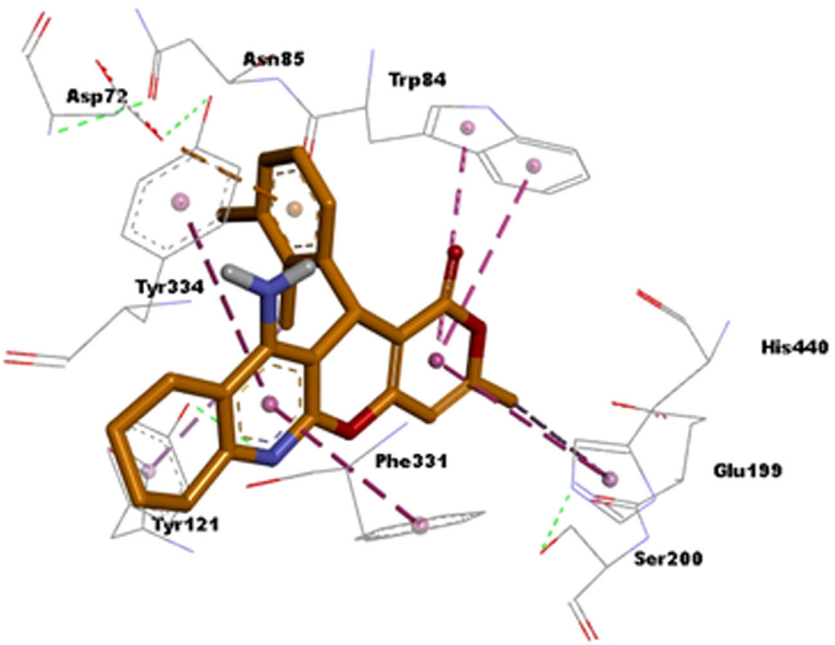

Figure 7. Representation of (*S*)-enantiomer (orange) of compound **6f** interacting with residues in AChE.

on Bruker FT-400 (Germany), using TMS as an internal standard. The IR spectra were obtained on a Nicolet Magna FTIR 550 spectrometer (KBr disks). The elemental analysis was performed with an Elementar Analysensysteme GmbH Vario EL (Germany). The InChI codes and representative spectra of the investigated compounds are provided as Supporting Information.

*Procedure for the synthesis of 2-amino-4-aryl-7-methyl-5-oxo-4,5-dihydropyrano[4,3-b]pyran-3-carbonitriles **4a–o***

A mixture of 4-hydroxy-6-methyl-2*H*-pyran-2-one (**1**) (1 mmol), appropriate aldehyde **2** (1 mmol), malononitrile (**3**) (1 mmol), and DABCO (20 mol%) in EtOH (10 mL) was stirred at room temperature for 12 h. After completion of reaction (checked by TLC), the mixture was filtered off, washed with cold EtOH, and dried at 50–60°C to afford pure compounds **4**.

*Procedure for the synthesis of pyrano[3′,4′:5,6]pyrano[2,3-b]quinolinones **6a–o***

A mixture of compound **4** (1 mmol) and cyclohexanone (**5**) (2 mmol) was added to the suspension of $AlCl_3$ in dry DCE (2 mmol in 30 mL) and heated at reflux for 12–18 h. After completion of reaction (checked by TLC), mixture of H_2O/THF (1:1, 100 mL) was added to the mixture and it was basicified with NaOH (10%). The mixture was stirred at room temperature for 30 min, the crude product was extracted using CH_2Cl_2 (2×50 mL) and washed with brine (2×50 mL). The organic phase was dried (Na_2SO_4) and the solvent was evaporated under vacuum. All compounds were recrystallized from EtOH to obtain pure products **6**.

*11-Amino-3-methyl-12-phenyl-7,9,10,12-tetrahydro-1H,8H-pyrano[3′,4′:5,6]pyrano[2,3-b]quinolin-1-one (**6a**)*

Yield: 69%; white solid; m.p. > 250°C. IR (KBr): 3422, 3344, 2933, 1722, 1657 cm^{-1}. ^1H NMR ($CDCl_3$, 400 MHz): 1.84–1.87 (m, 4H, $2 \times CH_2$), 2.23 (s, 3H, CH_3), 2.27–2.40 (m, 2H, CH_2), 2.78–2.81 (m, 2H, CH_2), 4.15 (s, 2H, NH_2), 4.89 (s, 1H, H12), 6.05 (s, 1H, H4), 7.21–7.33 (m, 3H, H3′, H4′, H5′), 7.42 (dd, $J = 7.5$, 1.6 Hz, 2H, H2′, H6′). ^{13}C NMR ($CDCl_3$, 100 MHz): 19.9, 22.3, 22.5, 22.9, 32.5, 36.1, 99.1, 99.4, 101.6, 114.4, 127.5, 128.6, 128.7, 141.7, 150.9, 153.7, 154.4, 160.2, 161.7, 163.1. Anal. calcd. for $C_{22}H_{20}N_2O_3$: C, 73.32; H, 5.59; N, 7.77. Found: C, 73.11; H, 5.38; N, 7.61.

*11-Amino-12-(2-fluorophenyl)-3-methyl-7,8,9,10-tetrahydropyrano[3′,4′:5,6]pyrano[2,3-b]quinolin-1(12H)-one (**6b**)*

Yield: 87%; white solid; m.p. > 250°C. IR (KBr): 3446, 3369, 2946, 1722 cm^{-1}. ^1H NMR ($CDCl_3$, 400 MHz): 1.85–1.86 (m, 4H, $2 \times CH_2$), 2.23 (s, 3H, CH_3), 2.26–2.40 (m, 2H, CH_2), 2.78–2.81 (m, 2H, CH_2), 4.18 (s, 2H, NH_2), 4.85 (s, 1H, H12), 6.05 (s, 1H, H4), 7.07–7.31 (m, 4H, H3′, H4′, H5′, H6′). ^{13}C NMR ($CDCl_3$, 100 MHz): 20.0, 22.2, 22.4, 220.9, 29.4 (d, $J_{C-F} = 2.9$ Hz), 32.4, 98.2, 99.3, 100.4, 114.2, 115.5 (d, $J_{C-F} = 22.4$ Hz), 124.8 (d, $J_{C-F} = 3.2$ Hz), 128.8 (d, $J_{C-F} = 13.0$ Hz), 129.1 (d, $J_{C-F} = 8.6$ Hz), 130.6 (d, $J_{C-F} = 3.7$ Hz), 150.7, 153.4, 154.2, 160.3 (d, $J_{C-F} = 243.8$ Hz), 161.0, 162.1, 162.8. Anal. calcd. for $C_{22}H_{19}FN_2O_3$: C, 69.83; H, 5.06; N, 7.40. Found: C, 69.62; H, 5.21; N, 7.28.

*11-Amino-12-(4-fluorophenyl)-3-methyl-7,8,9,10-tetrahydropyrano[3′,4′:5,6]pyrano[2,3-b]quinolin-1(12H)-one (**6c**)*

Yield: 53%; white solid; m.p. > 250°C. IR (KBr): 3422, 3344, 2937, 2859, 1716, 1657 cm^{-1}. ^1H NMR ($CDCl_3$, 400 MHz): 1.84–1.85 (m, 4H, $2 \times CH_2$), 2.23 (s, 3H, CH_3), 2.26–2.39 (m, 2H, CH_2), 2.78–2.81 (m, 2H, CH_2), 4.11 (s, 2H, NH_2), 4.89 (s, 1H, H12), 6.05 (s, 1H, H4), 6.98 (d, $J = 8.5$ Hz, 2H, H3′, H5′), 7.39 (dd, $J = 8.5$, 5.5 Hz, 2H, H2′, H6′). ^{13}C NMR ($CDCl_3$, 100 MHz): 19.9, 22.2, 22.5, 22.9, 32.5, 32.3, 98.8, 99.4, 101.5, 114.5, 115.6 (d, $J_{C-F} = 22.4$ Hz), 130.2 (d, $J_{C-F} = 21.5$ Hz), 137.4 (d, $J_{C-F} = 3.4$ Hz), 150.8, 153.7, 154.6, 160.2, 160.4 (d, $J_{C-F} = 233.3$ Hz), 161.9, 163.2. Anal. calcd. for $C_{22}H_{19}FN_2O_3$: C, 69.83; H, 5.06; N, 7.40. Found: C, 70.00; H, 4.81; N, 7.51.

*11-Amino-12-(2-chlorophenyl)-3-methyl-7,8,9,10-tetrahydropyrano[3′,4′:5,6]pyrano[2,3-b]quinolin-1(12H)-one (**6d**)*

Yield: 79%; white solid; m.p. > 250°C. IR (KBr): 3481, 3369, 2924, 1712, 1644, 1612 cm^{-1}. ^1H NMR ($CDCl_3$, 400 MHz): 1.80–1.82 (m, 4H, $2 \times CH_2$), 2.24 (s, 3H, CH_3), 2.28–2.40 (m, 2H, CH_2), 2.75–2.77 (m, 2H, CH_2), 4.45 (s, 2H, NH_2), 5.33 (s, 1H, H12), 6.07 (s, 1H, H4), 7.35 (dd, $J = 7.5$, 2.0 Hz, 1H, H3′), 714 (td, $J = 7.5$, 2.0 Hz, 1H, H4′), 7.19 (td, $J = 7.5$, 2.0 Hz, 1H, H5′), 7.26 (dd, $J = 7.5$, 2.0 Hz, 1H, H6′), 7.35 (dd, $J = 7.5$, 2.0 Hz, 1H, H3′). ^{13}C NMR ($CDCl_3$, 100 MHz): 20.0, 22.2, 22.4, 22.9, 32.4, 32.5, 98.6, 99.2, 101.0, 114.1, 127.7, 128.6, 129.5, 131.3, 133.1, 139.5, 151.0, 153.5, 154.3, 160.8, 162.0, 162.7. Anal. calcd. for $C_{22}H_{19}ClN_2O_3$: C, 66.92; H, 4.85; N, 7.09. Found: C, 66.78; H, 4.63; N, 6.91.

*11-Amino-12-(4-chlorophenyl)-3-methyl-7,8,9,10-tetrahydropyrano[3′,4′:5,6]pyrano[2,3-b]quinolin-1(12H)-one (**6e**)*

Yield: 51%; white solid; m.p. > 250°C. IR (KBr): 3415, 3341, 2930, 1719, 1660 cm^{-1}. ^1H NMR ($CDCl_3$, 400 MHz): 1.84–1.85 (m, 4H, $2 \times CH_2$), 2.23 (s, 3H, CH_3), 2.28–2.39 (m, 2H, CH_2), 2.78–2.80 (m, 2H, CH_2), 4.10 (s, 2H, NH_2), 4.88 (s, 1H, H12), 6.05 (s, 1H, H4), 7.26 (d, $J = 8.4$ Hz, 2H, H3′, H5′), 7.35 (d, $J = 8.4$ Hz, 2H, H2′, H6′). ^{13}C NMR ($CDCl_3$, 100 MHz): 20.0, 22.2, 22.4, 22.9, 32.5, 35.4, 98.5, 99.4, 101.2, 114.5, 128.9, 130.0, 133.3, 140.1, 150.8, 153.6, 154.7, 160.3, 162.0, 163.0. Anal. calcd. for $C_{22}H_{19}ClN_2O_3$: C, 66.92; H, 4.85; N, 7.09. Found: C, 67.18; H, 4.71; N, 7.23.

*11-Amino-12-(2,3-dichlorophenyl)-3-methyl-7,8,9,10-tetrahydropyrano[3′,4′:5,6]pyrano[2,3-b]quinolin-1(12H)-one (**6f**)*

Yield: 62%; white solid; m.p. > 250°C. IR (KBr): 3487, 3372, 2940, 1710, 1645 cm^{-1}. ^1H NMR ($CDCl_3$, 400 MHz): 1.82–1.83 (m, 4H, $2 \times CH_2$), 2.23 (s, 3H, CH_3), 2.25–2.41 (m, 2H, CH_2),

2.71–2.81 (m, 2H, CH_2), 4.40 (s, 2H, NH_2), 5.37 (s, 1H, H12), 6.07 (s, 1H, H4), 7.13 (t, $J = 7.6$ Hz, 1H, H5′), 7.20 (d, $J = 7.6$ Hz, 1H, H6′), 7.34 (dd, $J = 7.6$, 1.6 Hz, 1H, H4′). ^{13}C NMR ($CDCl_3$, 100 MHz): 20.0, 22.2, 22.4, 22.9, 32.4, 35.3, 98.5, 99.1, 101.1, 114.2, 127.8, 129.5, 129.6, 131.5, 133.5, 141.9, 151.0, 153.4, 154.5, 160.9, 162.3, 162.6. Anal. calcd. for $C_{22}H_{18}Cl_2N_2O_3$: C, 61.55; H, 4.23; N, 6.53. Found: C, 61.38; H, 4.40; N, 6.71.

*11-Amino-3-methyl-12-(2-nitrophenyl)-7,8,9,10-tetrahydropyrano[3′,4′:5,6]pyrano[2,3-b]quinolin-1(12H)-one (**6g**)*
Yield: 75%; white solid; m.p. > 250°C. IR (KBr): 3462, 3363, 2933, 1713, 1651, 1608, 1527, 1351 cm^{-1}. ^{1}H NMR ($CDCl_3$, 400 MHz): 1.83–1.86 (m, 4H, 2 × CH_2), 2.20 (s, 3H, CH_3), 2.24–2.41 (m, 2H, CH_2), 2.79–2.80 (m, 2H, CH_2), 5.10 (s, 2H, NH_2), 5.73 (s, 1H, H12), 6.02 (s, 1H, H4), 7.26 (d, $J = 7.5$ Hz, 1H, H6′), 7.33 (t, $J = 7.5$ Hz, 1H, H4′), 7.35 (t, $J = 7.5$ Hz, 1H, H5′), 7.79 (d, $J = 7.5$ Hz, 1H, H3′). ^{13}C NMR ($CDCl_3$, 100 MHz): 20.0, 22.2, 225, 23.0, 30.2, 32.5, 96.9, 99.2, 101.2, 114.1, 123.7, 128.0, 131.2, 133.3, 136.8, 150.2, 151.5, 154.0, 154.8, 160.0, 162.4, 162.8. Anal. calcd. for $C_{22}H_{19}N_3O_5$: C, 65.18; H, 4.72; N, 10.37. Found: C, 65.30; H, 4.58; N, 10.51.

*11-Amino-3-methyl-12-(3-nitrophenyl)-7,8,9,10-tetrahydropyrano[3′,4′:5,6]pyrano[2,3-b]quinolin-1(12H)-one (**6h**)*
Yield: 69%; white solid; m.p. > 250°C. IR (KBr): 3483, 3391, 3091, 2937, 1707, 1530, 1302 cm^{-1}. ^{1}H NMR ($CDCl_3$, 400 MHz): 1.85–1.86 (m, 4H, 2 × CH_2), 2.24 (s, 3H, CH_3), 2.27–2.40 (m, 2H, CH_2), 2.80–2.82 (m, 2H, CH_2), 4.15 (s, 2H, NH_2), 5.03 (s, 1H, H12), 6.09 (s, 1H, H4), 7.48 (t, $J = 7.6$ Hz, 1H, H5′), 7.81 (dt, $J = 7.6$, 2.0 Hz, 1H, H6′), 8.09 (dt, $J = 7.5$, 2.0 Hz, 1H, H4′), 8.22 (t, $J = 2.0$ Hz, 1H, H2′). ^{13}C NMR ($CDCl_3$, 100 MHz): 20.0, 22.2, 22.4, 22.9, 32.5, 35.8, 97.1, 99.5, 100.5, 114.7, 122.6, 123.4, 129.5, 134.8, 143.7, 148.6, 150.6, 153.6, 155.2, 160.7, 162.5, 163.0. Anal. calcd. for $C_{22}H_{19}N_3O_5$: C, 65.18; H, 4.72; N, 10.37. Found: C, 65.27; H, 4.88; N, 10.18.

*11-Amino-3-methyl-12-(o-tolyl)-7,9,10,12-tetrahydro-1H,8H-pyrano[3′,4′:5,6]pyrano[2,3-b]quinolin-1-one (**6i**)*
Yield: 69%; white solid; m.p. > 250°C. IR (KBr): 3514, 3419, 2940, 1710 cm^{-1}. ^{1}H NMR ($CDCl_3$, 400 MHz): 1.80–1.82 (m, 4H, 2 × CH_2), 2.22 (s, 3H, CH_3), 2.24–2.35 (m, 2H, CH_2), 2.65 (s, 3H, CH_3), 2.75–2.77 (m, 2H, CH_2), 4.06 (s, 2H, NH_2), 5.04 (s, 1H, H12), 6.05 (s, 1H, H4), 7.12–7.25 (m, 4H, H3′, H4′, H5′, H6′). ^{13}C NMR ($CDCl_3$, 100 MHz): 19.5, 20.0, 22.3, 22.5, 22.8, 32.3, 33.2, 99.2, 100.0, 101.4, 114.5, 126.8, 127.3, 130.3, 131.0, 136.1, 140.0, 151.1, 153.4, 154.2, 160.4, 161.6, 163.0. Anal. calcd. for $C_{23}H_{22}N_2O_3$: C, 73.78; H, 5.92; N, 7.48. Found: C, 73.56; H, 6.21; N, 7.61.

*11-Amino-3-methyl-12-(m-tolyl)-7,9,10,12-tetrahydro-1H,8H-pyrano[3′,4′:5,6]pyrano[2,3-b]quinolin-1-one (**6j**)*
Yield: 80%; white solid; m.p. > 250°C. IR (KBr): 3487, 3443, 2933, 2859, 1731 cm^{-1}. ^{1}H NMR ($CDCl_3$, 400 MHz): 1.81–1.83 (m, 4H, 2 × CH_2), 2.21 (s, 3H, CH_3), 2.27–2.37 (m, 5H, CH_2, CH_3), 2.76–2.79 (m, 2H, CH_2), 4.16 (s, 2H, NH_2), 4.74 (s, 1H, H12), 6.05 (s, 1H, H4), 7.02 (d, $J = 7.0$ Hz, 1H, H6′), 7.15–7.22 (m, 2H, H4′, H5′), 7.28 (s, 1H, H2′). ^{13}C NMR ($CDCl_3$, 100 MHz): 19.9, 21.4, 22.3, 22.5, 22.9, 32.4, 36.0, 99.3, 99.4, 101.7, 114.4, 125.8, 128.3, 128.5, 129.2, 138.5, 141.7, 151.0, 153.6, 154.3, 160.1, 161.6, 163.1. Anal. calcd. for $C_{23}H_{22}N_2O_3$: C, 73.78; H, 5.92; N, 7.48. Found: C, 73.60; H, 5.78; N, 7.24.

*11-Amino-3-methyl-12-(p-tolyl)-7,9,10,12-tetrahydro-1H,8H-pyrano[3′,4′:5,6]pyrano[2,3-b]quinolin-1-one (**6k**)*
Yield: 66%; white solid; m.p. > 250°C. IR (KBr): 3419, 3341, 2937, 2853, 1716, 1660 cm^{-1}. ^{1}H NMR ($CDCl_3$, 400 MHz): 1.82–1.84 (m, 4H, 2 × CH_2), 2.21 (s, 3H, CH_3), 2.27–2.38 (m, 5H, CH_2, CH_3), 2.77–2.80 (m, 2H, CH_2), 4.16 (s, 2H, NH_2), 4.74 (s, 1H, H12), 6.04 (s, 1H, H4), 7.10 (d, $J = 8.0$ Hz, 2H, H3′, H5′), 7.30 (d, $J = 8.0$ Hz, 2H, H2′, H6′). ^{13}C NMR ($CDCl_3$, 100 MHz): 19.9, 21.1, 22.3, 22.5, 22.9, 32.5, 35.6, 99.3, 99.4, 101.8, 114.4, 128.5, 129.5, 137.2, 138.8, 150.9, 153.7, 154.3, 160.0, 161.6, 163.1. Anal. calcd. for $C_{23}H_{22}N_2O_3$: C, 73.78; H, 5.92; N, 7.48. Found: C, 73.94; H, 6.11; N, 7.62.

*11-Amino-12-(4-methoxyphenyl)-3-methyl-7,9,10,12-tetrahydro-1H,8H-pyrano[3′,4′:5,6]pyrano[2,3-b]quinolin-1-one (**6l**)*
Yield: 74%; white solid; m.p. > 250°C. IR (KBr): 3434, 3351, 3159, 2943, 2841, 1726, 1654, 1611 cm^{-1}. ^{1}H NMR ($CDCl_3$, 400 MHz): 1.81–1.85 (m, 4H, 2 × CH_2), 2.20 (s, 3H, CH_3), 2.25–2.39 (m, 2H, CH_2), 2.77–2.80 (m, 2H, CH_2), 3.76 (s, 3H, OCH_3), 4.13 (s, 2H, NH_2), 4.84 (s, 1H, H12), 6.04 (s, 1H, H4), 6.82 (d, $J = 8.4$ Hz, 2H, H3′, H5′), 7.33 (d, $J = 8.4$ Hz, 2H, H2′, H6′). ^{13}C NMR ($CDCl_3$, 100 MHz): 19.9, 22.3, 22.5, 22.9, 32.5, 35.2, 55.2, 99.3, 99.4, 101.8, 114.1, 114.4, 129.7, 133.8, 150.9, 153.7, 154.3, 158.8, 159.9, 161.6, 163.1. Anal. calcd. for $C_{23}H_{22}N_2O_4$: C, 70.75; H, 5.68; N, 7.17. Found: C, 70.57; H, 5.81; N, 6.94.

*11-Amino-3-methyl-12-(3,4,5-trimethoxyphenyl)-7,9,10,12-tetrahydro-1H,8H-pyrano[3′,4′:5,6]pyrano[2,3-b]quinolin-1-one (**6m**)*
Yield: 79%; white solid; m.p. > 250°C. IR (KBr): 3474, 3381, 2940, 1722 cm^{-1}. ^{1}H NMR ($CDCl_3$, 400 MHz): 1.85–1.86 (m, 4H, 2 × CH_2), 2.23 (s, 3H, CH_3), 2.26–2.40 (m, 2H, CH_2), 2.77–2.80 (m, 2H, CH_2), 3.79–3.80 (s, 9H, 3 × OCH_3), 4.18 (s, 2H, NH_2), 4.85 (s, 1H, H12), 6.05 (s, 1H, H4), 6.62 (s, 2H, H2′, H6′). ^{13}C NMR ($CDCl_3$, 100 MHz): 19.9, 22.3, 22.5, 22.9, 32.5, 36.3, 56.3, 60.7, 98.9, 99.5, 101.5, 105.9, 114.4, 137.3, 137.4, 151.2, 153.4, 153.7, 154.5, 160.1, 161.7, 163.2. Anal. calcd. for $C_{25}H_{26}N_2O_6$: C, 66.65; H, 5.82; N, 6.22. Found: C, 66.48; H, 5.66; N, 6.50.

*11-Amino-12-(5-chloro-2-nitrophenyl)-3-methyl-7,9,10,12-tetrahydro-1H,8H-pyrano[3′,4′:5,6]pyrano[2,3-b]quinolin-1-one (**6n**)*
Yield: 54%; white solid; m.p. > 250°C. IR (KBr): 3483, 3394, 2943, 1716, 1648, 1515, 1345 cm^{-1}. ^{1}H NMR ($CDCl_3$, 400 MHz): 1.86–1.88 (m, 4H, 2 × CH_2), 2.22 (s, 3H, CH_3), 2.27–2.42 (m, 2H, CH_2), 2.80–2.82 (m, 2H, CH_2), 5.06 (s, 2H, NH_2), 5.75 (s, 1H, H12),

6.05 (s, 1H, H4), 7.18 (d, $J = 2.0$ Hz, 1H, H6′), 7.30 (dd, $J = 8.8$, 2.0 Hz, 1H, H4′), 7.77 (d, $J = 8.8$ Hz, 1H, H3′). ^{13}C NMR ($CDCl_3$, 100 MHz): 20.0, 22.2, 22.4, 22.9, 30.4, 32.5, 96.2, 99.3, 100.6, 114.3, 125.1, 128.4, 131.1, 138.9, 139.8, 146.9, 148.7, 151.4, 153.8, 155.2, 160.2, 162.7. Anal. calcd. for $C_{22}H_{18}ClN_3O_5$: C, 60.07; H, 4.12; N, 9.55 Found: C, 59.84; H, 4.32; N, 9.34.

*11-Amino-3-methyl-12-(thiophen-2-yl)-7,9,10,12-tetrahydro-1H,8H-pyrano[3′,4′:5,6]pyrano[2,3-b]quinolin-1-one (**6o**)*

Yield: 55%; white solid; m.p. > 250°C. IR (KBr): 3425, 3338, 2940, 1713, 1660, 1611 cm^{-1}. ^{1}H NMR ($CDCl_3$, 400 MHz): 1.84–1.88 (m, 4H, 2 × CH_2), 2.25 (s, 3H, CH_3), 2.31–2.43 (m, 2H, CH_2), 2.79–2.81 (m, 2H, CH_2), 4.26 (s, 2H, NH_2), 5.29 (s, 1H, H12), 6.05 (s, 1H, H4), 6.92 (dd, $J = 5.2$, 3.5 Hz, 1H, H4′), 7.15 (d, $J = 3.5$ Hz, 1H, H5′), 7.18 (dd, $J = 5.2$, 1.2 Hz, 1H, H3′). ^{13}C NMR ($CDCl_3$, 100 MHz): 20.0, 22.2, 22.5, 22.9, 30.7, 32.5, 98.7, 99.5, 100.2, 114.4, 125.2, 125.8, 126.5, 126.7, 145.2, 151.2, 154.8, 160.3, 161.9, 163.1. Anal. calcd. for $C_{20}H_{18}N_2O_3S$: C, 65.55; H, 4.95; N, 7.64. Found: C, 65.41; H, 5.18; N, 7.47.

Pharmacology

Reagents and chemicals

Acetylcholinesterase (AChE, E.C. 3.1.1.7, type V-S, lyophilized powder, from electric eel, 1000 units), butylcholinesterase (BChE, E.C. 3.1.1.8, from equine serum), acetylthiocholine iodide (ATCI), and 5,5-dithiobis-(2-nitrobenzoic acid) (DTNB) were purchased from Sigma–Aldrich. Potassium dihydrogen phosphate, dipotassium hydrogen phosphate, potassium hydroxide, and sodium hydrogen carbonate were obtained from Fluka. We followed our previous procedure for the evaluation of AChEI and BChEI activity based on Ellman's method. For this purpose, a solution of compound **6** in a mixture of DMSO (5 mL) and methanol (5 mL) was diluted in 0.1 M KH_2PO_4/K_2HPO_4 buffer (pH 8.0) to obtain final assay concentrations. All tests were conducted at 25°C and four different concentrations were evaluated for each compound in triplicate to obtain the range of 20–80% inhibition for AChE. *In vitro* anti-AChE activity was performed using a 96-well plate reader (BioTek ELx808). Each well included 50 μL potassium phosphate buffer (KH_2PO_4/K_2HPO_4, 0.1 M, pH 8), 25 μL sample dissolved in 50% methanol and 50% DMSO and 25 μL enzyme (final concentration 0.22 U/mL in buffer). They were preincubated for 15 min at room temperature and 125 μL DTNB (3 mM in buffer) was added to each plate. Characterization of the hydrolysis of ATCI catalyzed by AChE was performed spectrometrically at 405 nm followed by the addition of substrate (ATCI 3 mM in water). The change in absorbance was measured at 405 nm after 15 min. The IC_{50} values were determined graphically from inhibition curves (log inhibitor concentration vs. percent of inhibition). A control experiment was performed under the same conditions without inhibitor and the blank contained buffer, water, DTNB, and substrate. The described method was also used for BChE inhibition assay.

Kinetic studies of AChE inhibition

Estimates of the inhibition model and inhibition constant K_i, reciprocal plots of 1/*V* versus 1/[S] were obtained using different concentrations of the substrate, acetylthiocholine. For this purpose, experiments were performed similar to enzyme inhibition assay [20]. The rate of enzymatic reaction was obtained with different concentrations of inhibitor (0, 0.24, 0.47, and 0.93 μM). For each experiment, reaction was started by adding substrate (acetylthiocholine) and progress curves were recorded at 405 nm over 2 min. Next, double reciprocal plots (1/*v* vs. 1/[s]) were made using the slopes of progress curves to obtain the type of inhibition. Slopes of these reciprocal plots were then plotted against the concentration of compound **6f** in a weighted analysis, and K_i was determined as the intercept on the negative *x*-axis. All rate measurements were performed in triplicate and data analysis was performed with Microsoft Excel 2013.

BACE1 enzymatic assay

Compound **6f** was evaluated for the related BACE-1 inhibitory activity using a fluorescence resonance energy transfer (FRET) assay with recombinant human BACE-1 and quenched fluorescent peptide substrate based on the Swedish mutant APP sequence (SEVNLDAEFK). FRET-based enzymatic kit was purchased from Invitrogen (former Pan Vera corporation, Madison, WI) and the assay was carried out according to the manufacturers' instructions (Invitrogen, http://tools.invitrogen.com/content/sfs/manuals/L0724.pdf) using a multi-plate spectrofluorometer instrument (recording fluorescence at 544 nm excitation and 590 nm emission wavelengths) (BMG LABTECH, Polar star, Germany) [20].

Neuroprotection assay

PC12 cell line was purchased from the Pasteur Institute of Iran. Cells were cultivated in DMEM supplemented with 10% fetal calf serum, 5% horse serum, and antibiotics (100 units/mL penicillin, 100 μg/mL streptomycin). To induce neuronal differentiation, PC12 cells were re-suspended using trypsin/EDTA (0.25%) and seeded in 96-well culture plate (3000 cells/well) and cultured for 1 week in differentiation medium (DMEM + 2% horse serum + NGF (100 ng/mL) + penicillin and streptomycin). To evaluate the effect of drugs on survival rate of neurons, the culture medium was changed to NGF free medium and different concentrations of candidate drugs (10, 50, 100 μM) were applied on cells. Quercetin (50 μM) was used as a positive control. Drugs were diluted into DMEM and added to each well in the volume of 10 μL. Three hours later, induction of ROS mediated apoptosis was initiated by adding the H_2O_2 (400 μM) to their medium and after 12 h, MTT assay was performed. MTT solution (5 mg/mL) was added to each well in a volume of 10 μL, and 3 h later the culture medium was replaced with 100 μL of DMSO. Absorbance at 545 nm was determined for each well using an ELISA reader. Each experiment was performed in four replicates. All culture media and supplements were purchased from Gibco.

ARCH PHARM
Archiv der Pharmazie

Docking study

Docking simulations for compound **6f** were carried out by Autodock Vina (AV) 1.1.1 program [26]. For this purpose, the pdb structure of 1EVE was retrieved from the Brookhaven protein database (http://www.rcsb.org). Then, the water molecules and inhibitor were removed and enzyme.pdbqt was prepared by Autodock Tools (ver 1.5.4) with default parameters. The compound **6f** and its 3D structure were generated by MarvineSketch 5.8.3, 2012 and then ligand. pdbqt provided by Autodock Tools (ver 1.5.4). The Autodock Vina parameters were set as follow; box size: $40 \times 40 \times 40$ Å, the center of box: $x = 2.576$, $y = 65.277$, $z = 67.033$ (geometrical center of co-crystallized ligand), the exhaustiveness: 10, and the other parameters were left unchanged. The calculated geometries were ranked in terms of free energy of binding and the best pose was selected for further analysis. Molecular visualizations were performed by Discovery Studio 4.0 Client software (Accelrys, Inc., San Diego, CA) [18].

This research has been supported by a grant from the Research Council of Tehran University of Medical Sciences with project no. 93-03-92-26151.

The authors have declared no conflicts of interest.

References

[1] M. Prince, J. Jackson, *World Alzheimer Disease Report*, Alzheimer's Disease International, London **2009**, pp. 25–46.
[2] E. J. Mufson, S. E. Counts, S. E. Perez, S. D. Ginsberg, *Expert. Rev. Neurother*. **2008**, *8*, 1703–1718.
[3] R. T. Bartus, R. L. Dean, B. Beer, A. S. Lippa, *Science* **1982**, *217*, 408–414.
[4] S. Darvesh, D. A. Hopkins, C. Geula, *Nature Rev. Neurosci*. **2003**, *4*, 131–138.
[5] S. Darvesh, D. A. Hopkins, C. Geula, *Nat. Rev. Neursci*. **2003**, *4*, 131–138.
[6] H. Tago, T. Maeda, P. L. McGeer, H. Kimura, *J. Comp. Neurol*. **1992**, *325*, 301–312.
[7] E. Giacobini, *Neurochem. Int*. **1998**, *32*, 413–419.
[8] R. A. Armstrong, *Int. J. Alzheimers Dis*. **2011**, *2011*, 630865.
[9] G. B. Irvine, O. M. El-Agnaf, G. M. Shankar, D. M. Walsh, *Mol. Med*. **2008**, *14*, 451–464.
[10] N. C. Inestrosa, A. Alvarez, M. C. Dinamarca, T. Pérez-Acle, M. Colombres, *Curr. Alzheimer Res*. **2005**, *2*, 301–306.
[11] D. J. Selkoe, *Nature* **1999**, *399*, A21–A31.
[12] E. Heilbronn, *Acta Chem. Scand*. **1961**, *15*, 1386–1390.
[13] Tacrine. Drugs in Clinical Trials. Alzheimer Research Forum, http://www.alzforum.org/drg/drc/detail.asp?id = 90.
[14] M. I. Rodríguez-Franco, M. I. Fernández-Bachiller, C. Pérez, B. Hernández-Ledesma, B. Bartolomé, *J. Med. Chem*. **2006**, *49*, 459–462.
[15] S. Butini, E, Guarino, G. Campiani, M. Brindisi, S. S. Coccone, I. Fiorini, E. Novellino, T. Belinskaya, A. Saxena, S. Gemma, *Bioorg. Med. Chem. Lett*. **2008**, *18*, 5213–5216.
[16] E. Nepovimova, J. Korabecny, R. Dolezal, K. Babkova, A. Ondrejicek, D. Jun, V. Sepsova, A. Horova, M. Hrabinova, O. Soukup, N. Bukum, P. Jost, L. Muckova, J. Kassa, D. Malinak, M. Andrs, K. Kuca, *J. Med. Chem*. **2015**, *58*, 8985–9003.
[17] A. Romero, R. Cacabelos, M. J. Oset-Gasque, A. Samadi, J. Marco-Contelles, *Bioorg. Med. Chem. Lett*. **2013**, *23*, 1916–1922.
[18] M. Khoobi, F. Ghanoni, H. Nadri, A. Moradi, M. P. Hamedani, F. H. Moghadam, S. Emami, M. Vosooghi, R. Zadmard, A. Foroumadi, A. Shafiee, *Eur. J. Med. Chem*. **2015**, *89*, 296–303.
[19] M. Mahdavi, M. Saeedi, L. Gholamnia, S. A. B. Jeddi, R. Sabourian, A. Shafiee, A. Foroumadi, T. Akbarzadeh, *J. Heterocyclic Chem.*, in press. DOI: 10.1002/jhet.2594
[20] Z. Najafi, M. Saeedi, M. Mahdavi, R. Sabourian, M. Khanavi, M. B. Tehrani, F. H. Moghadam, N. Edraki, E. Karimpor-Razkenari, M. Sharifzadeh, A. Foroumadi, A. Shafiee, T. Akbarzadeh, *Bioorg. Chem*. **2016**, *67*, 84–94.
[21] M. Mohammadi-Khanaposhtani, M. Mahdavi, M. Saeedi, R. Sabourian, M. Safavi, M. Khanavi, A. Foroumadi, A. Shafiee, T. Akbarzadeh, *Chem. Biol. Drug Des*. **2015**, *86*, 1425.
[22] M. Mohammadi-Khanaposhtani, M. Saeedi, N. S. Zafarghandi, M. Mahdavi, R. Sabourian, E. K. Razkenari, H. Alinezhad, M. Khanavi, A. Shafiee, A. Foroumadi, T. Akbarzadeh, *Eur. J. Med. Chem*. **2015**, *92*, 799–806.
[23] M. Saeedi, M. Golipoor, M. Mahdavi, A. Moradi, H. Nadri, S. Emami, A. Foroumadi, A. Shafiee, *Arch. Pharm. Chem. Life Sci*. **2016**, *349*, 293–301.
[24] A. Rayatzadeh, M. Saeedi, M. Mahdavi, Z. Rezaei, R. Sabourian, M. H. Mosslemin, T. Akbarzadeh, A. Foroumadi, A. Shafiee, *Monatsh. Chem*. **2015**, *146*, 637–643.
[25] M. Saeedi, S. Ansari, M. Mahdavi, R. Sabourian, T. Akbarzadeh, A. Foroumadi, A. Shafiee, *Synth. Commun*. **2015**, *45*, 2311–2318.
[26] O. Trott, A. J. Olson, *J. Comput. Chem*. **2010**, *31*, 455–461.